Available at www.sciencedirect.com

ScienceDirect

journal homepage: www.elsevier.com/locate/carbon

Inkjet-defined field-effect transistors from chemical vapour deposited graphene

Sarah Hurch [a,b,1], *Hugo Nolan* [a,b], *Toby Hallam* [a,*], *Nina C. Berner* [a], *Niall McEvoy* [a], *Georg S. Duesberg* [a,b]

[a] *Centre for Research on Adaptive Nanostructures and Nanodevices (CRANN), Trinity College Dublin, Dublin 2, Ireland*

[b] *School of Chemistry, Trinity College Dublin, Dublin 2, Ireland*

ARTICLE INFO

Article history:
Received 26 July 2013
Accepted 27 January 2014
Available online xxxx

ABSTRACT

In this work, inkjet printing methods are used to create graphene field effect transistors with mobilities up to 3000 $cm^2 V^{-1} s^{-1}$. A commercially-available chromium-based ink is used to define the device channel by inhibiting chemical vapour deposition of graphene in defined regions on a copper catalyst. We report on the patterned graphene growth using optical and electronic microscopy, Raman spectroscopy and X-ray photoelectron spectroscopy. Silver nanoparticle ink is used to create electrical contacts to the defined graphene regions. The resulting devices were characterised by electrical transport measurements at room temperature. As a result we are able to fabricate high-performance graphene field effect transistors entirely defined by a commercial inkjet printer with channel lengths of 50 μm.

1. Introduction

Printed electronics is an evolving field, with improvements and developments in both techniques and materials used being reported regularly [1]. Inkjet printing is a simple printing method that can be used in versatile applications with materials such as metal nanoparticles, organometallics and polymers [2]. It is an economic process that requires minimum amounts of material and energy. Though inkjet printing might not be able to compete with conventional silicon micro-fabrication methods (e.g. lithography) when it comes to minimum feature size, it is very well suited for the fabrication of any kind of bigger features and many different products such as sensors, solar cells, display backplanes, electronic packaging and RF antennae have already been successfully fabricated by inkjet printing [3]. Inkjet printing is not only valuable in the production of prototypes but is also up-scalable for mass production and gives access to the fabrication of devices on a multitude of substrates, such as crystalline solids, glass or even plastics as high temperatures or harsh chemicals can be avoided. However, a disadvantage of this technique is that the types of material that may be printed generally offer poor electronic properties with polymeric semiconductor inks generally exhibiting mobilities under 1 $cm^2 V^{-1} s^{-1}$ [4,5].

One solution that has been pursued is to take the superior transport properties of carbon nanotubes (CNTs) and graphene and use them as an ink for printing. Inkjet printed transistors made of CNTs with mobilities up to 50 $cm^2 V^{-1} s^{-1}$ have been reported [6] and chemically exfoliated graphene

* *Corresponding author:* Fax: +353 (1)896 4628.
E-mail address: hallamt@tcd.ie (T. Hallam).
[1] Present address: Institute of Chemical Technologies and Analytics, Vienna University of Technology, Getreidemarkt 9/164, 1060 Wien, Austria.

http://dx.doi.org/10.1016/j.carbon.2014.01.063
0008-6223/

flake inks have demonstrated mobilities of up to 95 $cm^2 V^{-1} s^{-1}$ [7]. Unfortunately, the very nature of graphene and CNT inks limits their effectiveness due to the series resistance of many connections between the individual particles. Such inks annul many of graphene's superior electronic properties such as a high room temperature mobility (for standard transfer 4000–5000 $cm^2 V^{-1} s^{-1}$ have been reported [8]) and extremely large surface to volume ratio [9]. These properties of graphene may generally only be accessed via mechanically exfoliated [10], epitaxial [11] or chemical vapour deposition (CVD) [12] routes. Due to low throughput and extreme cost, the former two methods can be discounted but CVD graphene promises a low cost high throughput route to graphene.

Many different methods of producing graphene patterns of CVD graphene have been reported [13–15]. A widespread approach is to grow a continuous graphene sheet and later decompose specific areas. These methods, though, tend to decrease the quality of the graphene layer [13], and are limited to flat surfaces and a sometimes restrictive chemical environment associated with the technique. Another way of patterning graphene is to restrict growth to defined areas. This can either be achieved by pre-shaping a pattern of catalytic growth substrate (usually copper) on an inert basis substrate [16] or by physically blocking the growth in certain catalyst areas. We have used this latter method of blocking graphene growth in certain regions of a copper catalyst by ink-jet printing.

This work shows for the first time the use of commercially available chromium-based ink to define graphene growth patterns on a copper CVD catalyst. Microscopic and spectroscopic techniques were used to characterise the graphene patterns in conjunction with electrical device measurements. Electrical devices were fabricated by transfer of the prepatterned channels to insulating substrate and printing electrical contacts using a silver nanoparticle-based ink. In this way, graphene field effect transistors (GFETs) were created with minimal impact on the graphene channel, as all post growth structuring steps are avoided. Due to the low temperatures involved and the fact that no aggressive chemicals are required, this production route makes flexible, transparent electronics possible using inexpensive materials and fabrication techniques. While in this work we have used a lab scale technique for transfer of the structured graphene regions to a substrate there are a host of transfer techniques for achieving this that are more commercially viable [17,18]. It is envisaged that a combination of inkjet patterned CVD graphene and high speed roll-to-roll film transfer will be a powerful combination for graphene electronics.

2. Experimental setup

2.1. Pre-patterning of catalytic site of copper

A negative of the desired graphene pattern was designed and this inverse pattern was printed onto the Cu foil with a FUJIFILM Dimatix DMP 2831 printer. STAEDTLER® Lumocolor® permanent marker black ink was used without any further treatments to form a continuous film that prevented the growth in the coloured areas.

2.2. Growth

Graphene was grown via CVD on Cu foils in a hot wall quartz tube vacuum furnace. Substrates were heated to 1035 °C in 50 sccm hydrogen. After an annealing step of 1 h, 10 sccm CH_4 and 2.5 sccm H_2 were introduced to the furnace for 20 min. After this the CH_4 flow was turned down and the furnace force-cooled to room temperature.

2.3. Transfer

After growth the Cu foil was subjected to mild sonication in acetone to remove the pyrolysed residue of the ink layer. A standard procedure was employed to transfer the graphene films to SiO_2 wafers whereby a handling layer of poly-methyl methacrylate (PMMA) was spun onto the graphene. The Cu foil was etched using ammonium persulfate (APS) solution, the graphene/PMMA film transferred to the target substrate and the PMMA layer dissolved in acetone.

2.4. Ag contact printing

To form contact leads to the graphene SunTronic® silver conductive nanoparticle ink was printed with a FUJIFILM Dimatix DMP 2831 printer. The silver nanoparticle patterns were sintered for 10 min at 180 °C in air to form conductive features.

2.5. Analytics

Raman scans were performed with a Witec Alpha 300 R using a 532 nm laser. Scanning electron microscopy (SEM) was executed with a Carl Zeiss Ultra SEM. X-ray photoelectron spectroscopy (XPS) measurements were carried out in ultra-high vacuum, using unmonochromatised Al Kα X-rays from a PSP twin anode source and a VG Scientific CLAM2 energy analyser.

2.6. Electrical measurements

For the acquisition of transport data the GFETs were always measured at room temperature using a 4 electrode configuration (as depicted in Fig. 4a). In this setup a constant current of 100 μA is applied between the outer two electrodes and the changing voltage between the inner two electrodes is measured during source-drain voltage sweeps (−70 to 70 V).

3. Results and discussion

In Fig. 1 a schematic of the device fabrication process is shown. An inverse pattern of the required graphene geometry was designed on a computer [Pattern Design] and subsequently printed in marker ink onto copper foils [Prepatterning]. Graphene was grown on the foils by a CVD process [CVD]. The graphene features were transferred to an arbitrary substrate, in this study to Si/SiO_2 wafers [Transfer]. Contact leads were printed onto the graphene with silver nanoparticle ink [Contacting] and the nanoparticles were then sintered at 180 °C for 10 min to form conductive silver features [Sintering].

Please cite this article in press as: Hurch S et al. Inkjet-defined field-effect transistors from chemical vapour deposited graphene. Carbon (2014), http://dx.doi.org/10.1016/j.carbon.2014.01.063

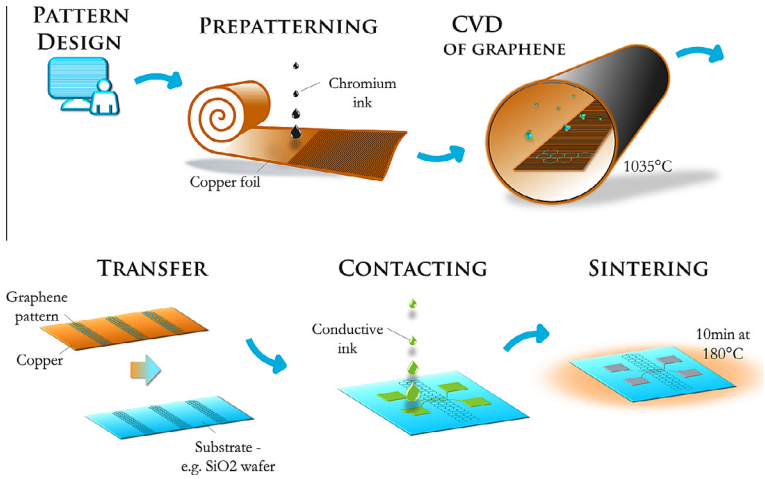

Fig. 1 – Flow chart of the fabrication of GFETs; the inverse pattern is designed on a computer, the pattern is printed on copper foil with an inkjet printer, graphene is grown via CVD on the patterned foil, the graphene features are transferred to an arbitrary substrate, contact leads are inkjet printed onto the graphene with silver nanoparticle ink, the ink is sintered at 180 °C to improve its conductivity. (A colour version of this figure can be viewed online.)

With this process any desired graphene pattern can be produced by providing the printer with the corresponding instructions. This is shown in Fig. 2a–d. Fig. 2a shows a copper foil with the negative of the research group logo printed on it. Fig. 2b shows the foil after being subjected to CVD growth. Areas which were not previously inked appear to be blank but are covered with graphene. Other areas are coated with carbon residues. The majority of these ink residues can be removed by mild sonication in acetone without damaging the graphene (Fig. 2c). After the transfer to a Si/SiO_2 substrate, the logo made of graphene is clearly discernible from the formerly inked areas. In these areas small amounts of amorphous carbon residues are still present and are visible due to the hue in the background in Fig. 2d.

The resolution of patterning is limited by the size of the droplets formed by the inkjet printer. The standard width of a printed marker ink line on copper foils was ~70 μm. With optimisation of the printing technique graphene features down to 10 μm were achieved by controlling the ink line spacing (see Fig. 3a). However, such small features show poor reproducibility. As previously described, graphene only grows in non-inked areas, so control of the spacing between adjacent ink lines allows control over the width of graphene features. For the fabrication of GFETs in this study graphene strips of ~50 μm width were produced.

The ink was analysed to discern information about the mechanism by which graphene growth was suppressed. To this end, a drop of ink was dried on a SiO_2 wafer and analysed using XPS. A survey spectrum showed the elemental composition of the ink as well as spectral contributions from the SiO_2 substrate (see Fig. S2). It was determined that the ink consists of organic material (C, O, N) with chromium also present. This is in keeping with the available information about the ink as published by the manufacturer, which describes the ink as a combination of pigment material, organic resin binder and alcohol-based solvent. The presence of Cr was attributed to the pigment material. SEM and energy dispersive X-ray spectroscopy (EDX) confirm the presence of chromium in the areas were growth was prevented. Studies towards the mechanism preventing the growth showed that not only does chromium act as a passivation layer that blocks the growth but it also poisons growth in its immediate vicinity (see Fig. S1).

Some works have shown the conversion of solid precursors to graphene upon annealing. In this study, it is likely that the presence of a solid carbon source enriches the carbon content of the vapour phase. However, in this study it was not seen to significantly affect the graphene growth [19]. Further, organic resins are known to pyrolyse under similar conditions to form a glassy carbon layer [20]. Raman spectroscopy

Fig. 2 – (a) Cu foil that has been prepatterned with the inverse pattern; dark (inked) areas will not grow graphene, bare copper will; (b) the same foil after CVD growth; (c) after mild sonication and (d) graphene pattern transferred to SiO_2 wafer. (A colour version of this figure can be viewed online.)

Please cite this article in press as: Hurch S et al. Inkjet-defined field-effect transistors from chemical vapour deposited graphene. Carbon (2014), http://dx.doi.org/10.1016/j.carbon.2014.01.063

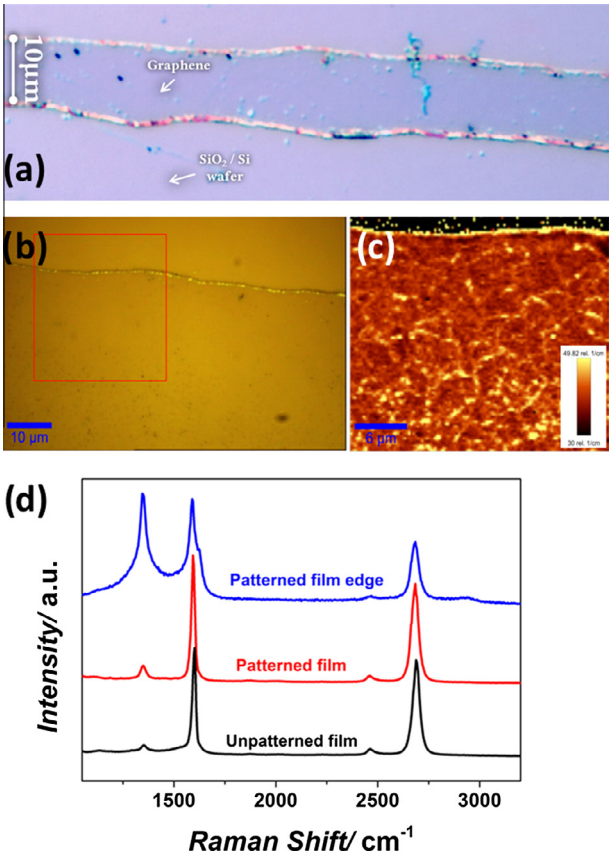

Fig. 3 – (a) Optical image of a 10 μm graphene feature, (b) optical image of the edge of a graphene feature and (c) a Raman map of the area in the square showing the 2D peak FWHM, (d) Raman spectra of unpatterned graphene (black), Raman spectra of the graphene in (c) red, Raman spectra of the edge of the graphene film in (c) blue. (A colour version of this figure can be viewed online.)

of ink residues after CVD growth showed highly disordered graphitic carbon (see Fig. S3). We tentatively assign the selective growth on the copper foil to a combination of metallic chromium and an amorphous carbon layer, provided by the ink, preventing the graphene growth during CVD.

In the uncovered catalyst areas graphene growth was observed [21]. The quality of the produced graphene features was analysed using optical microscopy, SEM and Raman spectroscopy. Fig. 3b shows an optical image of the edge of a graphene feature on SiO_2. It is clearly defined and shows a slight line edge roughness. Fig. 3c depicts a map of Raman scans of the red square indicated in Fig. 3b. Scanning Raman spectroscopy takes many discrete scans across the surface of a sample and gives information on the variation of the Raman spectrum across a given area of the sample. The map shows the full width half maximum (FWHM) of the 2D Raman peak, which gives information on the number of graphene layers. A continuous film of monolayer graphene with small bilayer islands is observed. The sharp 2D peak can be fitted with a single Lorentzian function affirming the presence of predominantly monolayer graphene [22].

We would like to comment here that the ratio of amplitudes of the G and 2D peaks shown in Fig. 3d to not conform to one of the typical requirements for monolayer graphene (i.e. G:2D < 0.5). this is because the position of the confocal plane during Raman imaging can heavily influence the ratio of the G and 2D peaks. Fig. S4 shows the variation of peak intensities for a variety of focal positions highlighting the variability of the peak ratio. The ratio of G:2D peak heights is also affected by extrinsic doping from polymer residue. Suk et al. have shown that the G:2D ratio can be larger than 0.5 for sufficient levels of polymer residue [8]. In this work, the more reliable peak shape of the 2D peak has been invoked to determine layer number.

The edges of the graphene features are well defined and show an increase in the D peak intensity which is associated with structural changes at the edge of the film [23]. Averaging over the scans confirms that the grown graphene

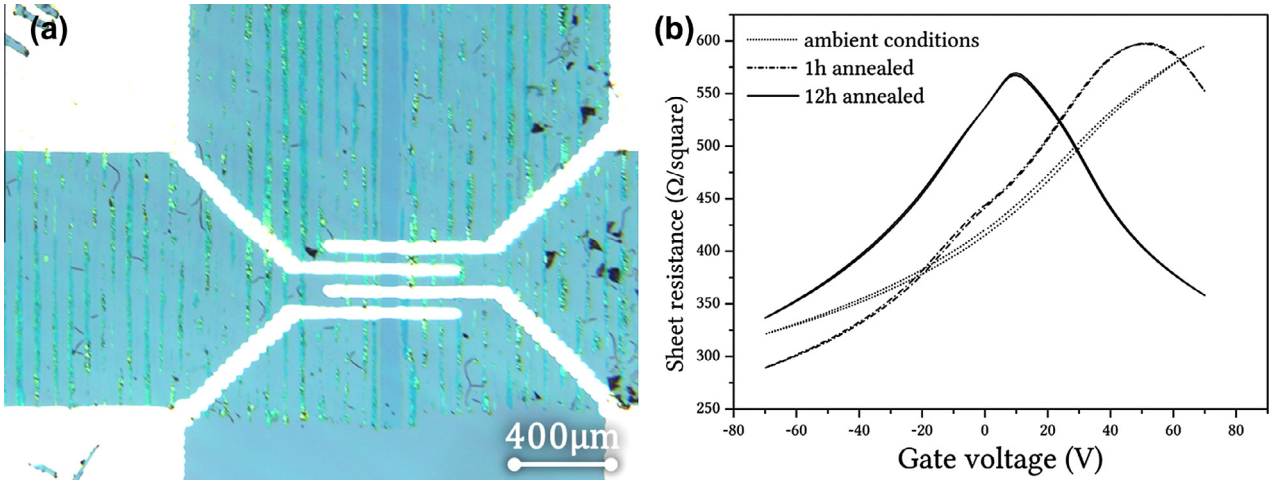

Fig. 4 – (a) Photograph of an inkjet printed CVD GFET; the active channel can be seen between the inner two electrodes and has in this device a dimension of 70–50 μm (L:W) (b) comparison of the measured sheet resistance vs. gate voltage, of such a device in ambient conditions [black], after a 1 h vacuum anneal [blue] and after a subsequent 12 h vacuum anneal [turquoise]; this device was fabricated to channel dimensions of 50–38 μm (L:W). (A colour version of this figure can be viewed online.)

Please cite this article in press as: Hurch S et al. Inkjet-defined field-effect transistors from chemical vapour deposited graphene. Carbon (2014), http://dx.doi.org/10.1016/j.carbon.2014.01.063

is comparable to growth on unpatterned copper foils with the same CVD procedure (see Fig. 3d).

In order to create functional GFETs graphene stripes were transferred onto highly doped Si wafers with a thermally grown 300 nm SiO_2 top layer and a gold covered back to form a bottom gate. The stripes had lengths up to 1 cm and widths of 50 μm. With the inbuilt camera of the printing set-up the samples were aligned in the printer. Electrodes were printed with silver nanoparticle ink on top of the graphene to form devices such as the one shown in the optical image in Fig. 4a. The line width of printed ink is dependent on the wettability of the substrate. Silver line widths of 50 μm on bare SiO_2 and of 40 μm on CVD grown graphene transferred to SiO_2 were realised. After sintering the silver nanoparticles at 180 °C fully functioning GFETs were produced (also see the black curve in Fig. 4b [ambient conditions]). The measured devices were defined with a channel length [*L*] of 50 μm and variable channel widths [*W*] giving a *W*:*L* ratios between 0.76 and 2.2. On these devices the influence of polymer residues from the used transfer process was observed. Polymer residues remaining on the graphene surface can hugely impact its electrical properties and either a chemical treatment [8], vacuum exposure [24] or a vacuum anneal [25] can be used to remove these residues. In this study after the first set of electrical measurements the samples were subjected to a vacuum anneal, carried out at 500 K under high-vacuum conditions ($\sim 10^{-6}$ mbar), to further improve their electrical performance. The sheet resistance vs. the gate voltage of one such a device is depicted in Fig. 4b. The unannealed device measured in ambient conditions showed the characteristics of highly doped graphene. A Dirac point at ~50 V was typically measured for anneal times of 1 h. Longer anneals shifted the Dirac point down to nearly 10 V.

Electron mobilities of up to 2700 $cm^2 V^{-1} s^{-1}$ and hole mobilities of up to 3300 $cm^2 V^{-1} s^{-1}$ were calculated. Out of 6 fabricated devices the average carrier mobility was 2000 $cm^2 V^{-1} s^{-1}$. Both the Dirac point being close to charge neutrality and the high carrier mobilities underline the high quality of the graphene.

4. Summary

Catalyst patterning by printing allows any given graphene features to be grown down to the micrometre scale. Raman spectroscopy indicates that the crystallinity of the patterned films is comparable to unpatterned films. Furthermore, we have shown that it is possible to contact the high quality CVD grown graphene patterns by inkjet printing of conducting inks. In this manner GFETs have been produced using inkjet printing for both the pre-patterning of CVD graphene as well as the deposition of metallic contacts. Thus the processing techniques allow entire electronic devices to be fabricated without the use of lithographic patterning techniques, which are known to deteriorate the quality of graphene. The GFETs have mobilities up to 3300 $cm^2 V^{-1} s^{-1}$, the highest carrier mobilities reported for inkjet-defined devices. The scalability and low-cost associated with the printing processes opens a route towards the larger scale fabrication of cheap and flexible graphene-based electronic devices.

Acknowledgements

This work was supported by the SFI under Contracts No. 08/CE/I1432, 08/CE/I1432S, PI_10/IN.1/I3030 and by the EU under FP7-PPP Electrograph (Con. No. 266391) and NMP-ICT GRAFOL (Con. No. 285275). The authors thank Richard Coull of Hewlett Packard Ireland for assistance with inkjet printing and the AML for microscopy support.

Appendix A. Supplementary data

Supplementary data associated with this article can be found, in the online version, at http://dx.doi.org/10.1016/j.carbon.2014.01.063.

REFERENCES

[1] Tekin E, Smith PJ, Schubert US. Inkjet printing as a deposition and patterning tool for polymers and inorganic particles. Soft Matter 2008;4(4):703–13.
[2] Singh M, Haverinen HM, Dhagat P, Jabbour GE. Inkjet printing – process and its applications. Adv Mater 2010;22(6):673–85.
[3] Cummins G, Desmulliez MPY. Inkjet printing of conductive materials: a review. Circuit World 2012;38:193–213.
[4] Park SK, Jackson TN, Anthony JE, Mourey DA. High mobility solution processed 6,13-bis(triisopropylsilylethynyl) pentacene organic thin film transistors. Appl Phys Lett 2007;91(6):063514–6.
[5] Yan H, Chen Z, Zheng Y, Newman C, Quinn JR, Dotz F, et al. A high-mobility electron-transporting polymer for printed transistors. Nature 2009;457(7230):679–86.
[6] Ha M, Xia Y, Green AA, Zhang W, Renn MJ, Kim CH, et al. Printed, sub-3V digital circuits on plastic from aqueous carbon nanotube inks. ACS Nano 2010;4(8):4388–95.
[7] Torrisi F, Hasan T, Wu W, Sun Z, Lombardo A, Kulmala TS, et al. Inkjet-printed graphene electronics. ACS Nano 2012;6(4):2992–3006.
[8] Suk JW, Lee WH, Lee J, Chou H, Piner RD, Hao Y, et al. Enhancement of the electrical properties of graphene grown by chemical vapor deposition via controlling the effects of polymer residue. Nano Lett 2013;13(4):1462–7.
[9] Geim AK. Graphene: status and prospects. Science 2009;324(5934):1530–4.
[10] Novoselov KS, Geim AK, Morozov SV, Jiang D, Zhang Y, Dubonos SV, et al. Electric field effect in atomically thin carbon films. Science 2004;306(5696):666–9.
[11] Berger C, Song Z, Li T, Li X, Ogbazghi AY, Feng R, et al. Ultrathin epitaxial graphite: 2D electron gas properties and a route toward graphene-based nanoelectronics. J Phys Chem B 2004;108(52):19912–6.
[12] Li X, Cai W, An J, Kim S, Nah J, Yang D, et al. Large-area synthesis of high-quality and uniform graphene films on copper foils. Science 2009;324(5932):1312–4.
[13] Kumar S, Peltekis N, Lee K, Kim H-Y, Duesberg G. Reliable processing of graphene using metal etchmasks. Nanoscale Res Lett 2011;6(1):390.
[14] Wei D, Liu Y. Controllable synthesis of graphene and its applications. Adv Mater 2010;22(30):3225–41.
[15] Zhou Y, Loh KP. Making patterns on graphene. Adv Mater 2010;22(32):3615–20.
[16] Casey AH, Xiaojun W, Vince B, David S, Joshua AR. Substrate considerations for graphene synthesis on thin copper films. Nanotechnology 2012;23(13):135601.

[17] Bae S, Kim H, Lee Y, Xu X, Park J-S, Zheng Y, et al. Roll-to-roll production of 30-inch graphene films for transparent electrodes. Nat Nanotechnol 2010;5(8):574–8.
[18] Kang J, Hwang S, Kim JH, Kim MH, Ryu J, Seo SJ, et al. Efficient transfer of large-area graphene films onto rigid substrates by hot pressing. ACS Nano 2012;6(6):5360–5.
[19] Ruan G, Sun Z, Peng Z, Tour JM. Growth of graphene from food, insects, and waste. ACS Nano 2011;5(9):7601–7.
[20] Schreiber M, Lutz T, Keeley GP, Kumar S, Boese M, Krishnamurthy S, et al. Transparent ultrathin conducting carbon films. Appl Surf Sci 2010;256(21):6186–90.
[21] Kumar S, McEvoy N, Kim H-Y, Lee K, Peltekis N, Rezvani E, et al. CVD growth and processing of graphene for electronic applications. Phys Status Solidi B 2011;248(11):2604–8.
[22] Ferrari A, Meyer J, Scardaci V, Casiraghi C, Lazzeri M, Mauri F, et al. Raman spectrum of graphene and graphene layers. Phys Rev Lett 2006;97(18):187401.
[23] Tuinstra F, Koenig JL. Raman spectrum of graphite. J Chem Phys 1970;53(3):1126–30.
[24] Ni ZH, Wang HM, Luo ZQ, Wang YY, Yu T, Wu YH, et al. The effect of vacuum annealing on graphene. J Raman Spectrosc 2010;41(5):479–83.
[25] Pirkle A, Chan J, Venugopal A, Hinojos D, Magnuson CW, McDonnell S, et al. The effect of chemical residues on the physical and electrical properties of chemical vapor deposited graphene transferred to SiO_2. Appl Phys Lett 2011;99(12):122108.

Please cite this article in press as: Hurch S et al. Inkjet-defined field-effect transistors from chemical vapour deposited graphene. Carbon (2014), http://dx.doi.org/10.1016/j.carbon.2014.01.063